

GEOS 4310/5310 Lecture Notes: Unsaturated Flow

Dr. T. Brikowski

Fall 2011

Introduction

- good general online reference is Natural Resources Conservation Service Soil Survey Manual

Introduction

- increasingly important in hydrology because it is the link between the surface and the water table
- also because almost all solid waste disposal takes place above the water table (e.g. Yucca Mountain Nuclear Waste Repository)
- involves any water found between the ground surface and top of the capillary fringe
- unsaturated flow is also known as partially-saturated or *vadose zone* flow
- unsaturated zone pores are partially filled with water, i.e.₂

pores contain water + air; consequently water surface tension plays an important role in fluid movement (Fig. 1)

- more difficult to study and model than saturated flow, only recently addressed in great detail

Soil Makeup

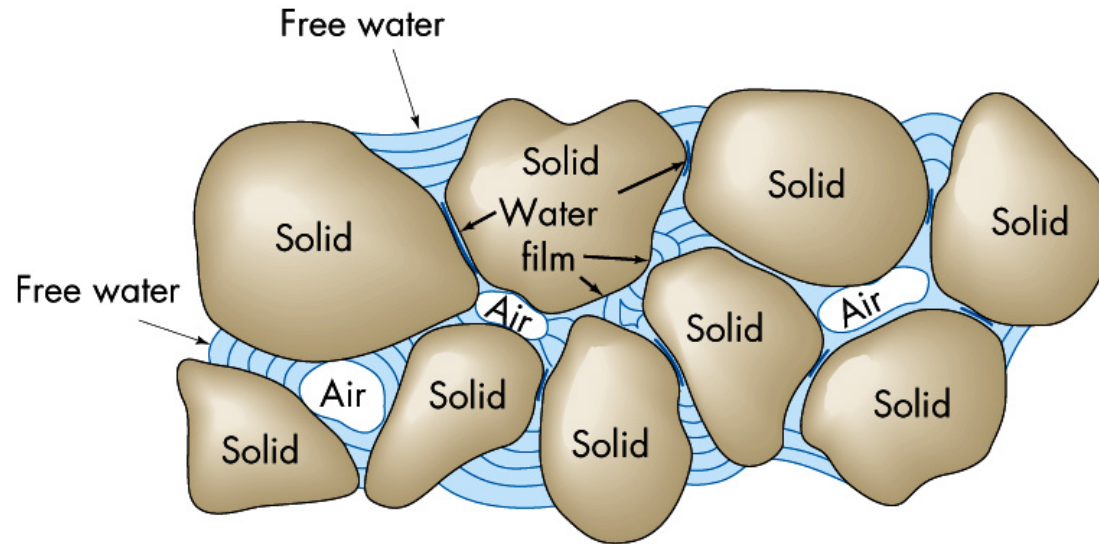


Figure 1: Air-water-particle relationships in soil [Fig. 17.7, Keller, 2011]. Changes in the distribution of air and water generally control soil behavior.

Unsaturated vs. Saturated Flow Regimes

Table 1: Comparison of saturated and unsaturated flow regimes Freeze and Cherry [after 1979, , p. 44]. Symbols: moisture content (volumetric) θ , porosity ϕ , pressure head ψ , P_{gage} gage pressure (relative to atmospheric, $P_{gage} = 0$ at the water table), air-entry pressure P_a , and hydraulic conductivity K .

Saturated	Unsaturated
Below water table	Above water table (and capillary fringe)
$\theta = \phi$	$\theta < \phi$
$P > P_a$	$P < P_a$
$P_{gage} > 0$	$P_{gage} < 0$
$\psi > 0$	$\psi < 0$
h measured with piezometer	h measured with tensiometer
$K \neq f(\theta)$	$K = K(\theta)$

Basic Soil Properties

Table 2: Soil volumetric and weight properties, after Keller [Fig. 3A, 2000].

Volume				Weight	
V total volume	V_v void volume	V_a air volume	Air	W_a	W
		V_w water volume	Water	W_w	
	V_s solid volume		Solid	W_s	

And porosity n or ϕ $= \frac{V_v}{V}$

volumetric water content θ_v $= \frac{V_w}{V}$
 $= \frac{\left(\frac{W - W_s}{\rho_w}\right)}{V}$

saturation R_s or S $= \frac{V_w}{V_v}$

Capillarity

Surface Tension

- arises because liquid molecules at the air-water interface are preferentially drawn away from the air by liquid-liquid bonds
- causes the air-water interface to be curved
- curves such that the surface area between the two phase is minimized [see also Hillel, 1980]
- similar tension arises along the interface between water and solid
- Minimum surface energy (tension) is achieved by balancing these two components

Capillary Rise

- study using capillary tube example (Fig. 2)
- solid-liquid interface
 - against glass (polar surface), water forms an acute angle (the wetting angle)
 - such an angle is sought by the water all around the water-tube interface
 - tries to form the water surface in the tube into a downward-pointing cone
- liquid-gas interface
 - air-water interface also seeks to be minimized (i.e. to be rounded) in center of tube

- draws the interface in the center of the tube upward
- lowers the water pressure in the tube, and in general water pressure inside a capillary tube is lower than atmospheric, by an amount equal to the total surface-tension

Capillary Tube

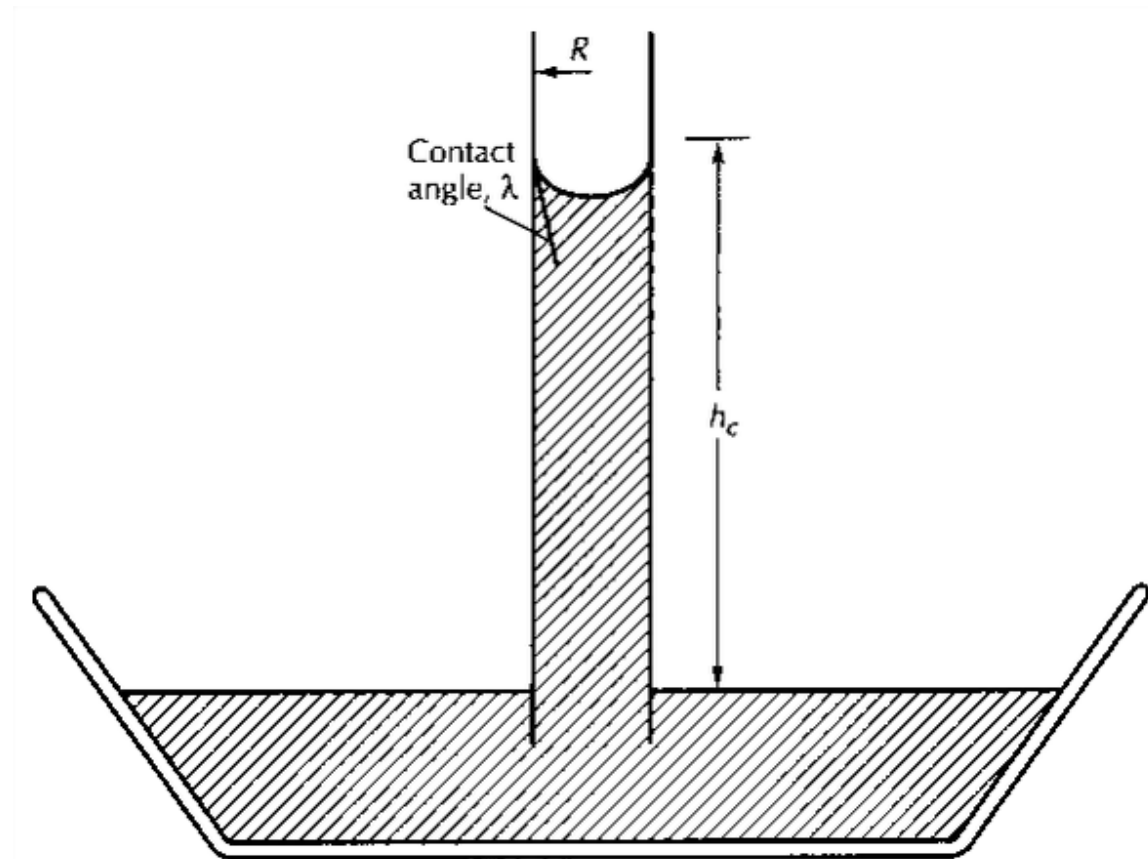


Figure 2: Capillary rise in a tube Fetter [Fig. 6.1, 2001].

Capillary Fringe

- Knowing the tube radius, surface tension and the wetting angle, the capillary rise (or fluid pressure) can be calculated [eqn. 6-15, Fetter, 2001]
- soils can be modeled as bundles of capillary tubes
- a *capillary fringe* forms above the water table, where pores are saturated but fluid pressure is negative

Moisture Balance

Soil Moisture Balance

- as in the saturated zone, a water (moisture) mass balance can be performed for the soil (Fig. 3–4)
- this is an important activity in agriculture, rangeland and forest management
- Definitions:
 - *field capacity* of soil: minimum soil moisture content resulting from pure gravity drainage [Fig. 6.5, Fetter, 2001]
 - *wilting point*: minimum soil moisture content produced by gravity drainage + plant evapotranspiration. Always lower than field capacity (Fig. 5)

- groundwater recharge cannot occur unless soil moisture content exceeds field capacity

Moisture Budget

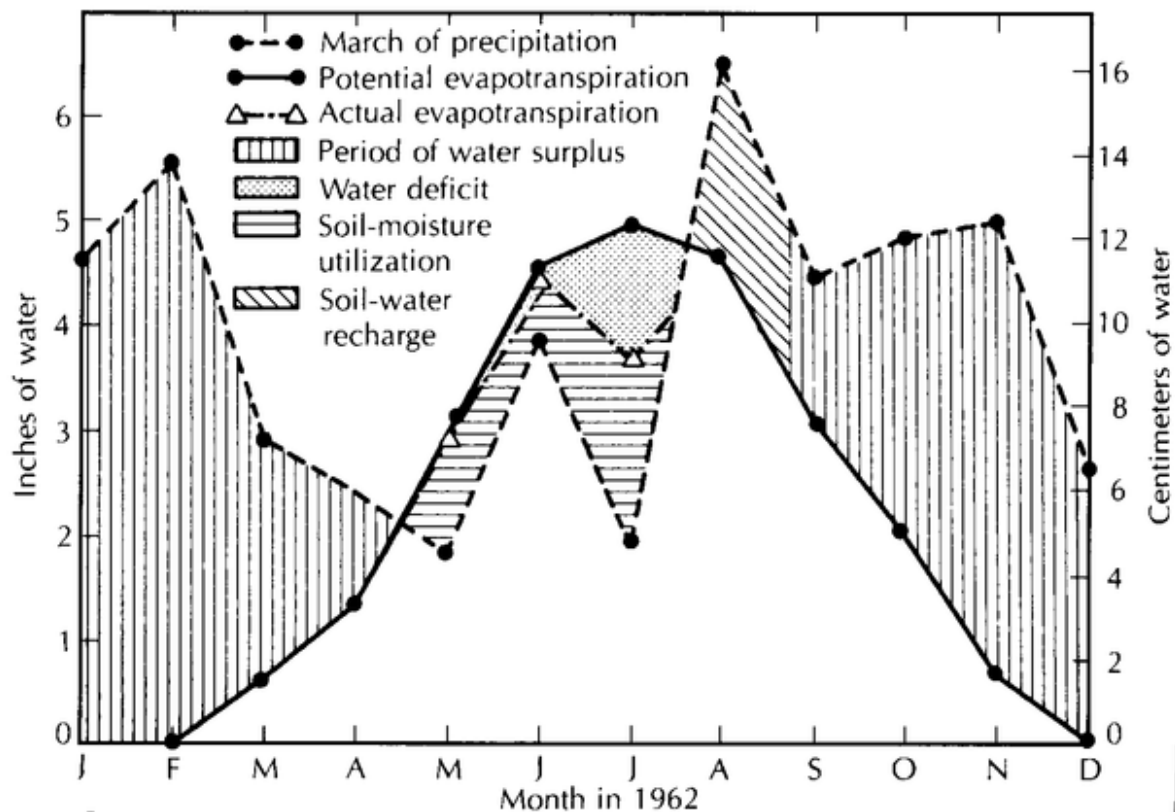


Figure 3: Soil moisture budget for a farm field Fetter [Fig. 6.3, 2001]. PET computed using Thornthwaite Method, actual ET computed.

Annual Moisture Variation

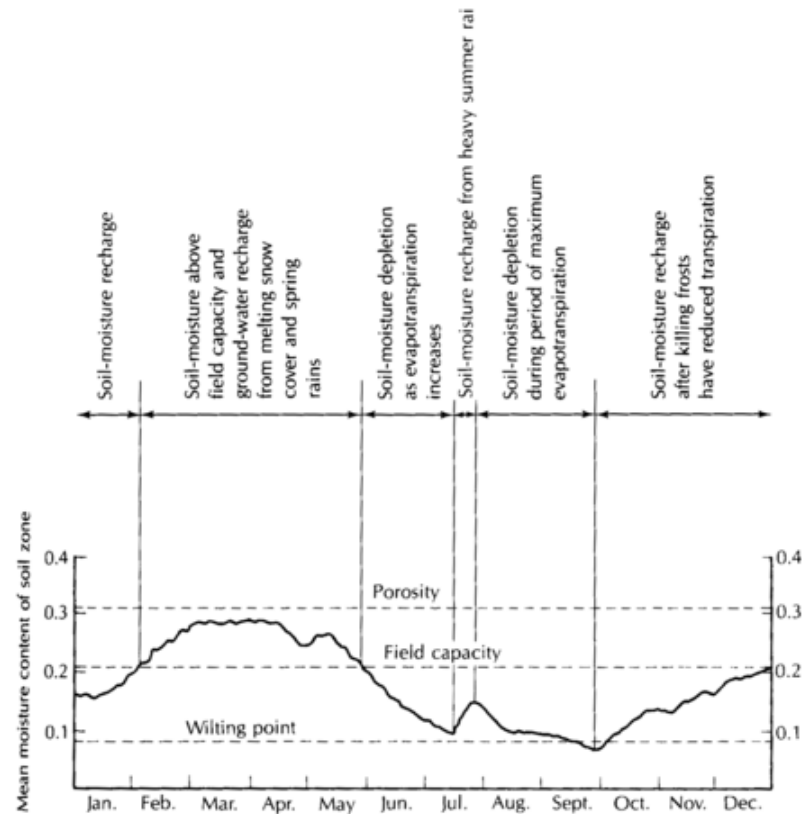


Figure 4: Hypothetical annual variation of soil moisture Fetter [Fig. 6.4, 2001]. Note especially groundwater and soil moisture recharge periods

Texture vs. Water Content

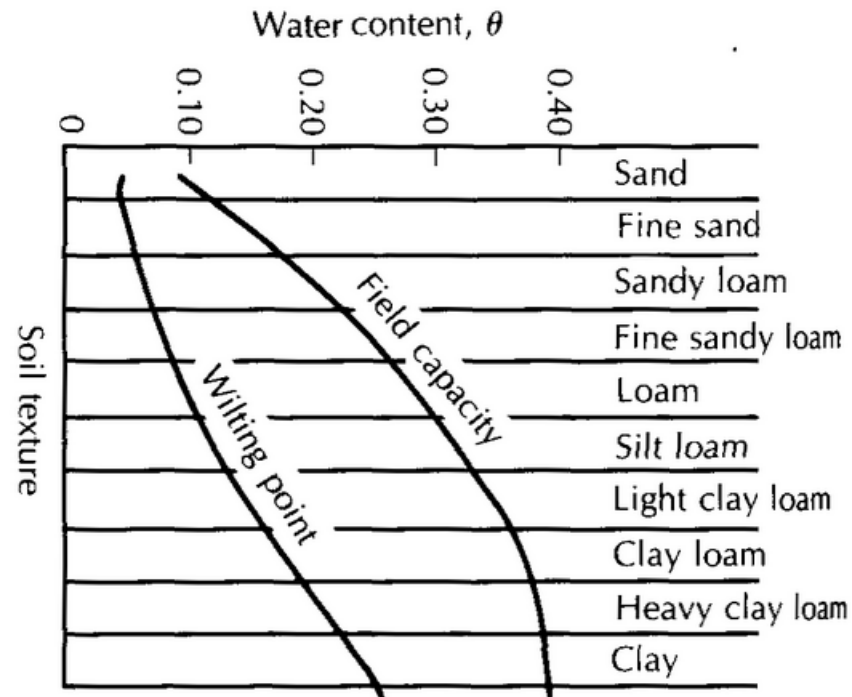


Figure 5: Dependence of water content on grain size. Field capacity is maximum storage possible under gravity drainage, wilting point is minimum storage under gravity drainage only. After Fetter [Fig. 6.5, 2001].

Pressure Head and Tension

- because of capillary forces, fluid pressure (or pressure head ψ) are generally negative (when given as gage pressures)
- soil scientists often refer to these as *suction* or *tension* head, and omit the negative sign. We won't do that in this class.
- fluid pressure and soil moisture content are directly related because of capillary forces

Moisture Content: Measurement

- laboratory: gravimetric analysis (wet then dry weighing of soil sample)
- field:
 - *tensiometer* (measure pressure directly, good for low-suction settings, Fig. 6)
 - resistance cells (*gypsum blocks*, dissolve in ~ 1 year, Fig. 7)
 - thermocouple *psychrometer*, good for high-suction settings (Fig. 8)
 - *TDR* or time domain reflectometry (Fig. 9)
 - * Sends signal down a pair of conductors (waveguides)

- * speed of wave depends on interaction with surroundings, determined by the dielectric constant of the soil
- * that varies directly with moisture content
- * same principle as ground-penetrating radar (GPR)
- * accurate, flexible, mildly expensive
- * most widely used is the Hydraprobe
- *neutron probe* (Fig. 10)
 - * Given a source of fast (high-energy) neutrons
 - * these interact with pore water producing slow (thermal) neutrons
 - * measuring thermal neutron density indicates moisture content
 - * expensive, accurate at all suctions, but risky (neutron source required)

Tensiometer



Figure 6: Tensiometer for measuring soil suction in moist settings. Tube is partly filled with water, low-permeability porous cup at bottom allows pressure equilibration with soil, pressure gauge measures suction (pore pressure relative to atmosphere). See also SoilMoisture Inc..

Gypsum Block Moisture Sensor

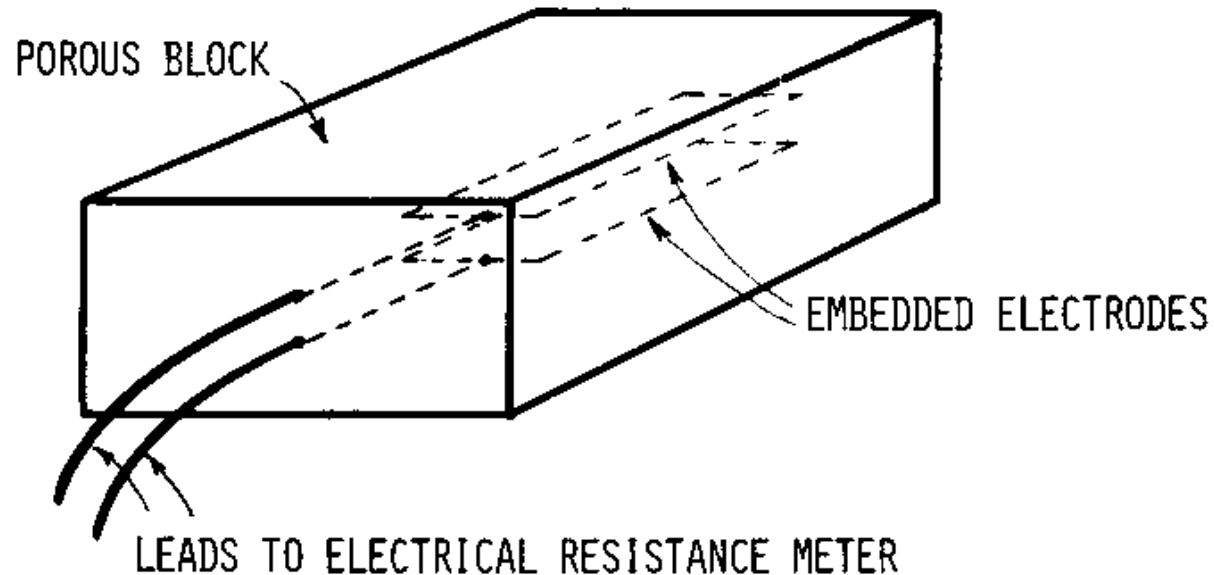


Figure 7: Gypsum (electrical resistance) block for measuring in-situ moisture content. Blocks equilibrate with soil, resistance of gypsum vs. moisture content known, and used to quantify moisture content. Blocks dissolve with time, leading to drift in measurements. After Hillel [Fig. 7.2, 1980]. See also SoilMoisture Inc..

Thermocouple Psychrometer

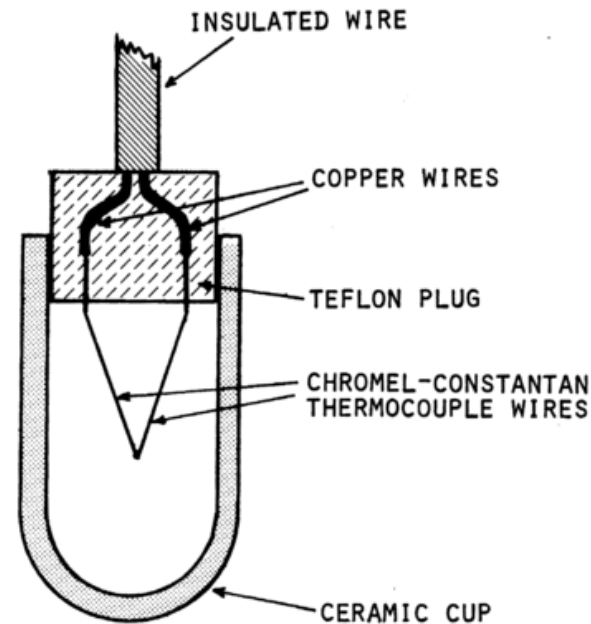


Figure 8: Thermocouple psychrometer for measuring in-situ soil moisture content. Functions by measuring relative humidity within porous ceramic cup, which essentially indicates saturation. Effective in moist and relatively dry settings, after Hillel [Fig. 7.13, 1980].

TDR Probe



Figure 9: Time-domain reflectometry probe. Signal propagates down probes, reflects from end, travel time is measured at top unit. See SoilMoisture, Inc. and TDR animation.

Neutron Probe

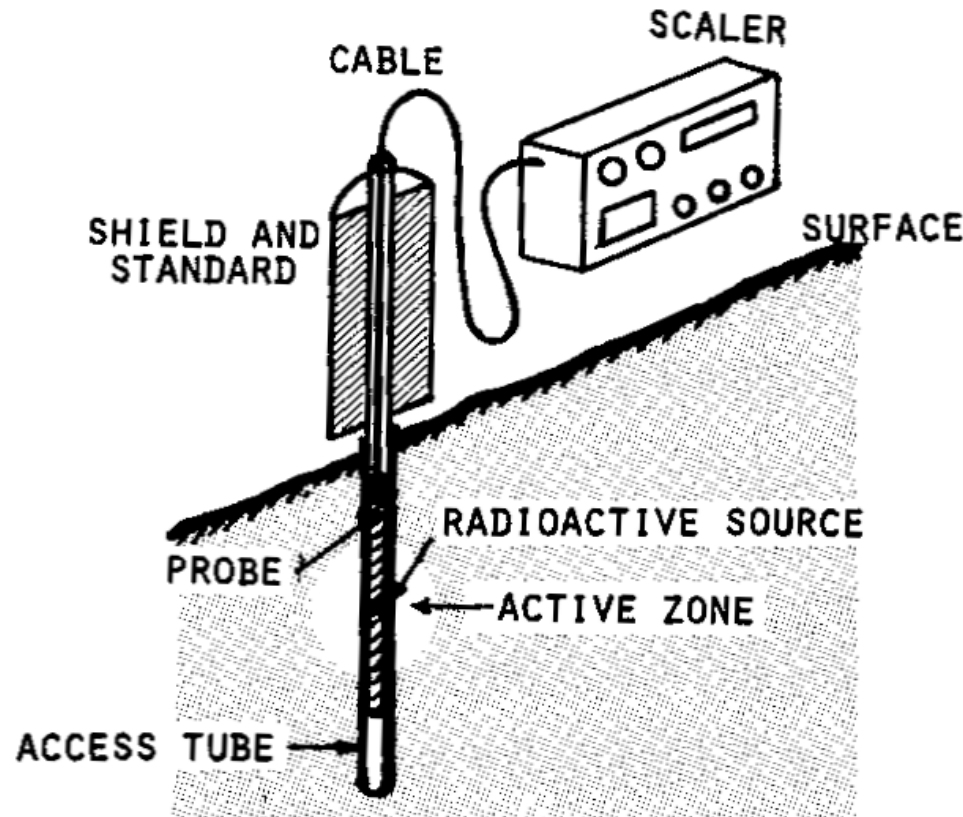


Figure 10: Neutron probe for measuring soil moisture, especially useful for vertical profiles in boreholes. After Hillel [Fig. 7.3, 1980].

Theory of Unsaturated Flow

Characteristic Curves

- the relationships between pressure head ψ , volumetric moisture content, and hydraulic conductivity, are typically described graphically via *characteristic curves* (Fig. 11).
- Moisture Retention Curve (Fig. 13)
 - moisture content θ can be measured for a soil held under varying pressure head ψ
 - this is plotted as a moisture retention curve [e.g. Fig. 6.7, Fetter, 2001].
 - two curves are generally found, depending on whether the sample is being progressively dried or wetted. This is hysteresis
 - air-entry value:

- * as a sample is gravity-drained from an initially saturated state, saturation changes little at first
- * eventually the saturation begins to change rapidly with little change in ψ , as pores begin emptying, and air becomes a continuous phase in the pores.
- * this occurs at the *air-entry value* ψ_a of pressure head, and the corresponding fluid pressure is the air-entry or bubbling pressure (Fig. 13)

- Hysteresis

- hysteresis generally means a multi-valued function (e.g. multiple values of θ are found for a given ψ , depending on the history of the sample)
- this phenomenon considerably complicates modeling of unsaturated flow

- Conductivity curve

- measured by fixing the sample θ and observing the water flow rate. Darcy's Law is used to obtain $K(\theta)$
- conductivity decreases as pressure declines (i.e. with decreasing saturation) because the water phase in the pores becomes poorly connected.
- when $\log K$ is plotted against ψ , the curves are quite similar to those for θ vs ψ (Fig. 14) or [e.g. Fig. 6.8 Fetter, 2001]
- large pores will drain more quickly, which can preferentially direct flow (e.g. in the matrix rather than fractures in fractured rock), or lead to surprising results (clay often has higher conductivity than sand or gravel at low water content) (Fig. 15)

Example Characteristic Curves

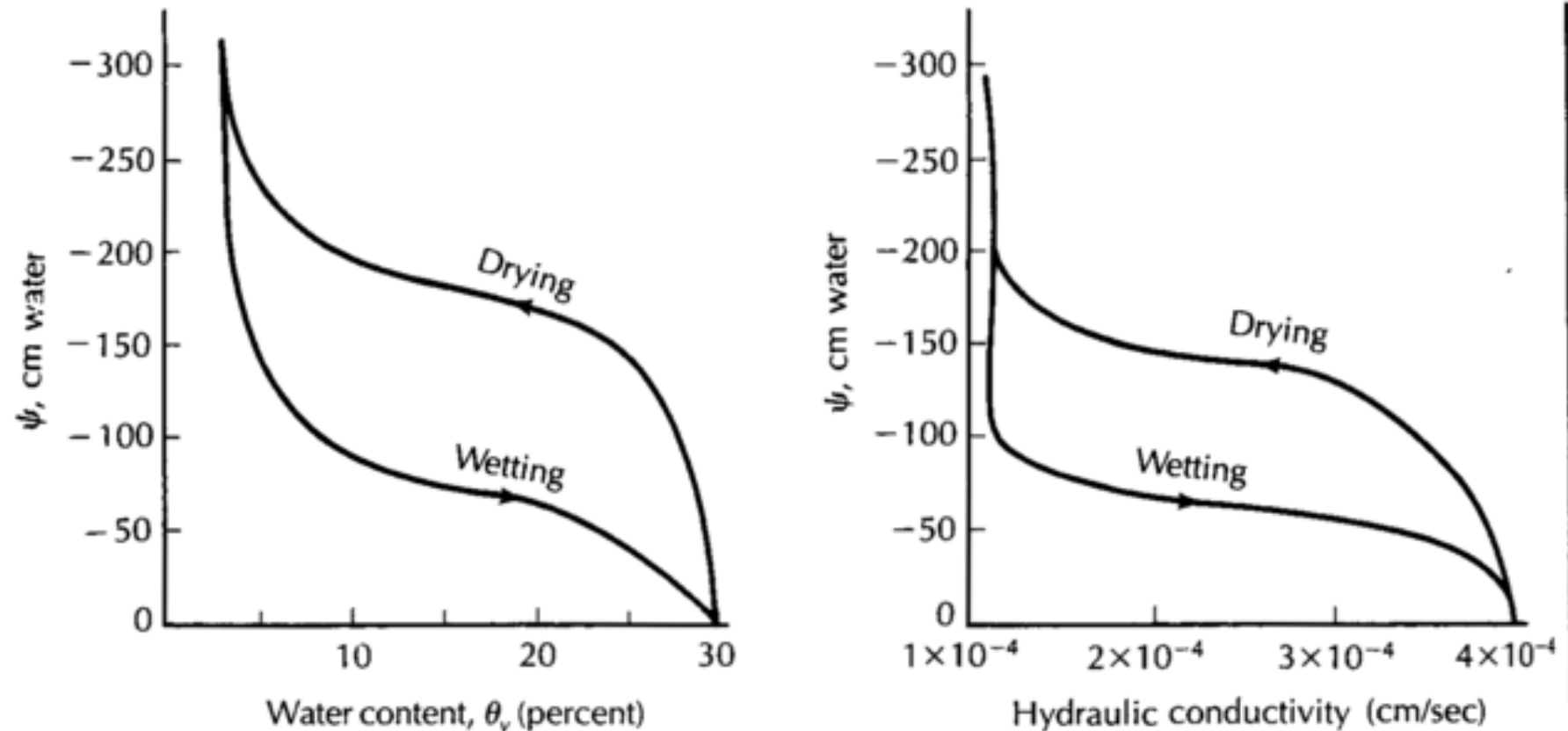


Figure 11: Idealized curves of tension head (ψ), hydraulic conductivity (K) and water content (θ) After Fetter [Fig. 6.8, 2001].

Moisture Retention vs. Grain Size

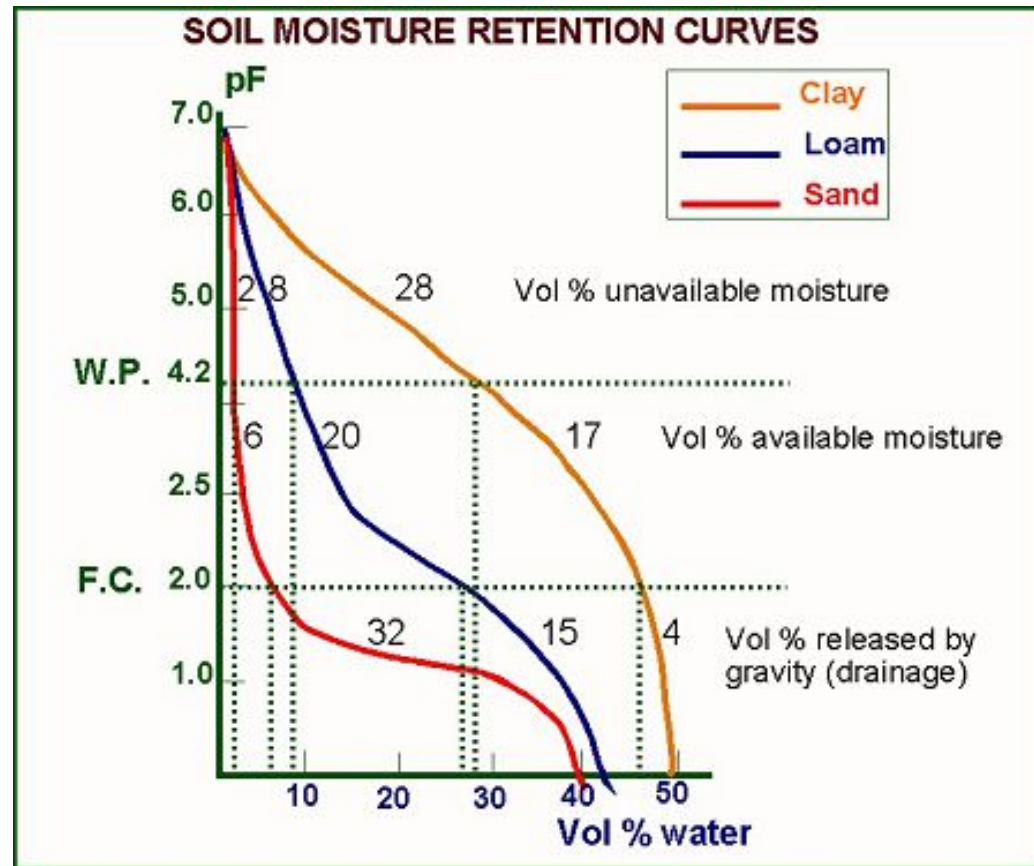


Figure 12: Available moisture vs. grain size, after soil saturation summary.

Water Content vs. P, Clay Loam

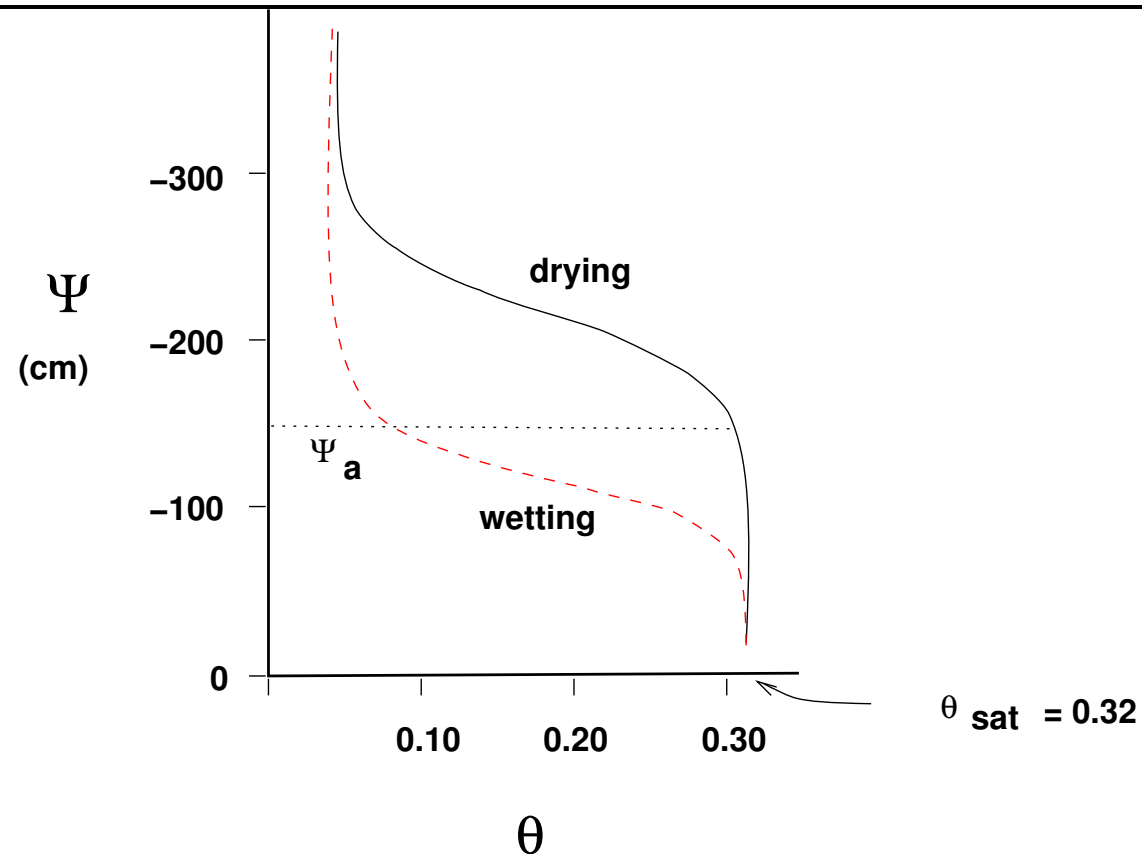


Figure 13: Schematic moisture retention curve showing typical relationship between pressure head ψ and moisture content θ in unsaturated materials. Hysteresis shown, where wetting curve always lies to the higher ψ side of the drying curve.

See also Fetter [Fig. 6.8, 2001] and Freeze and Cherry [Fig. 2.13, 1979].

K vs. Water Content, Clay Loam

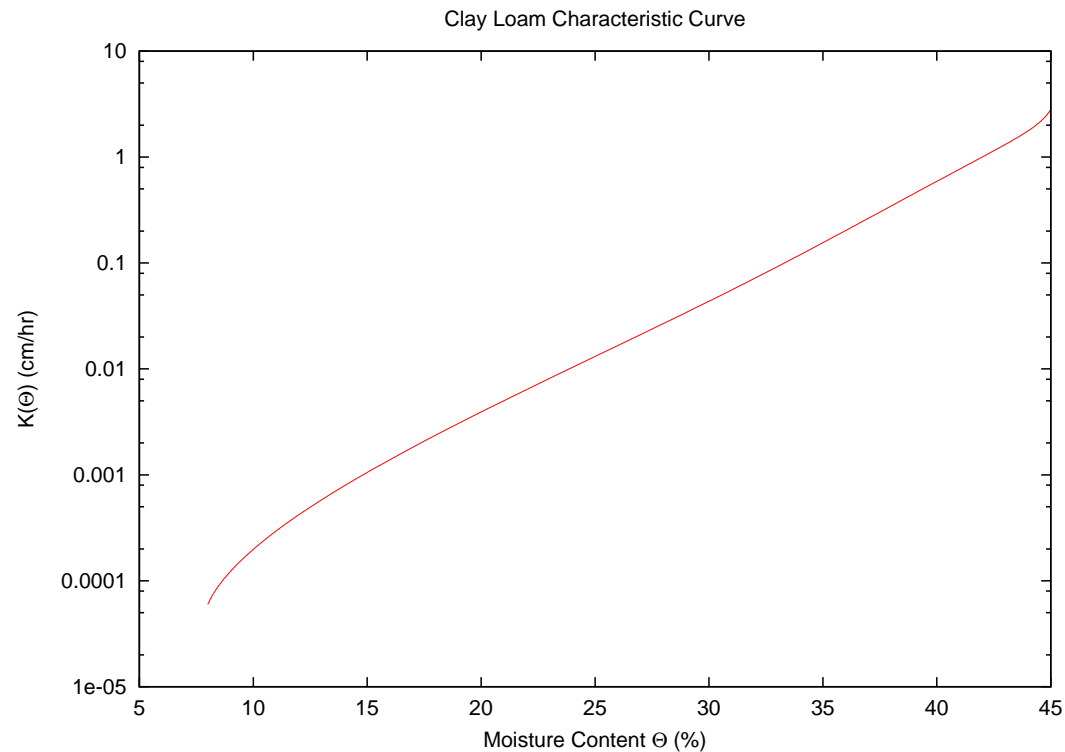


Figure 14: Schematic unsaturated conductivity curve showing typical relationship between moisture content θ and hydraulic conductivity (K) in unsaturated materials. See also Fetter [Fig. 6.8, 2001] and Freeze and Cherry [Fig. 2.13, 1979].

K vs. Grain Size

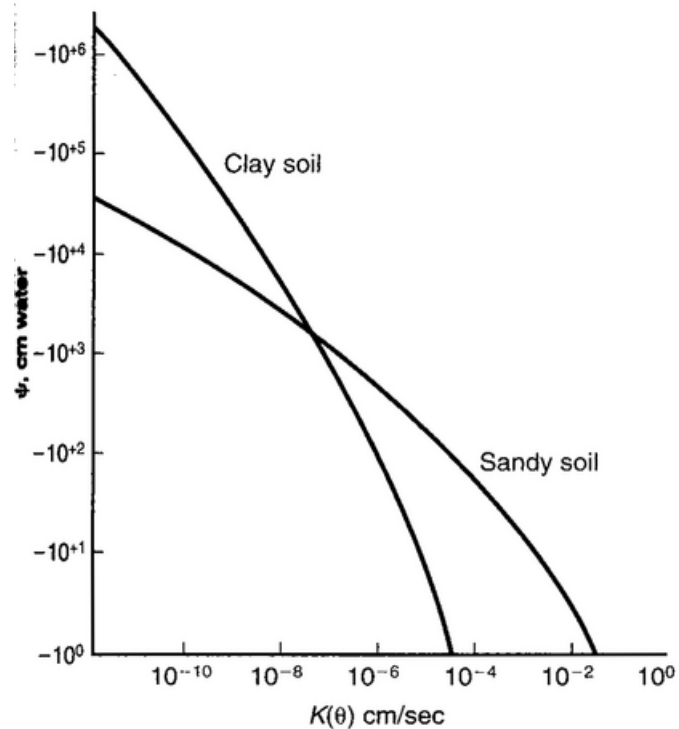


Figure 15: Dependence of hydraulic conductivity on water content and grain size. Note crossover where coarse sediments become more permeable at high water contents. After Fetter [Fig. 6.10, 2001].

Unsaturated Flow Equation

- head in the unsaturated zone is the sum of the elevation z and pressure head ψ , just as in the saturated zone
- the flow equation is different than the saturated case, since conductivity is a function of ψ or θ
- Flow Equation (AKA Richards Equation, the form below assumes $\nabla\psi \gg 1$)

$$\begin{aligned}\frac{\partial\theta}{\partial t} &= \nabla \cdot (K(\psi)\nabla\psi) \\ &= \frac{\partial}{\partial x} \left[K(\psi)\frac{\partial\psi}{\partial x} \right] + \dots\end{aligned}$$

- solution of this non-linear equation can be difficult, but a number of good numerical models are available (e.g. HYDRUS2D)

Infiltration Pulse

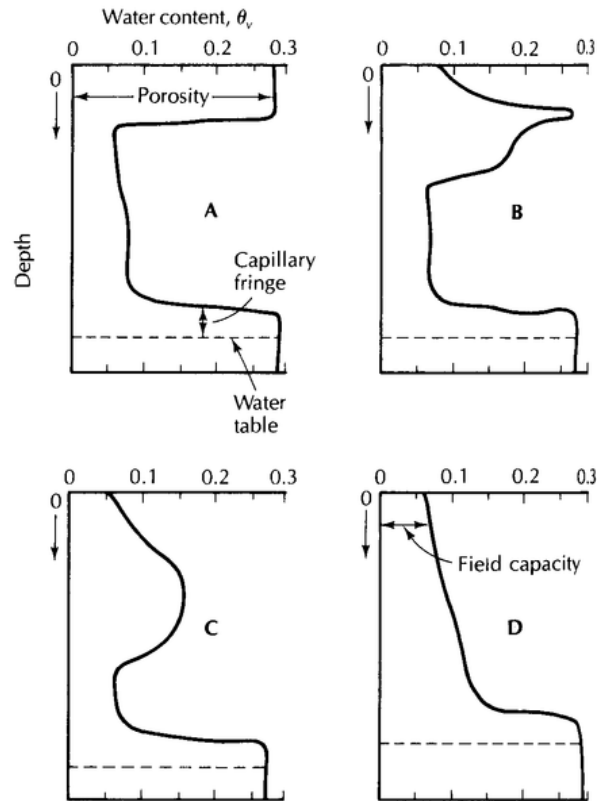


Figure 16: Downward movement of infiltration pulse in a soil, with porosity of 29% (i.e. $\theta = 0.29$ is full saturation. Field capacity is 0.06. After Fetter [Fig. 6.9, 2001].

Vertisols and Central Texas Hydrogeology

- Central Texas (primarily along the Edwards-Trinity groups) is characterized by *Vertisols*, a taxonomic soil group that exhibits shrink-swell behavior (Fig. 17)
- one well-studied site is Riesel, TX [USDA-ARS Grassland, Soil and Water Research Laboratory, Allen et al., 2005]

Vertisols in Texas

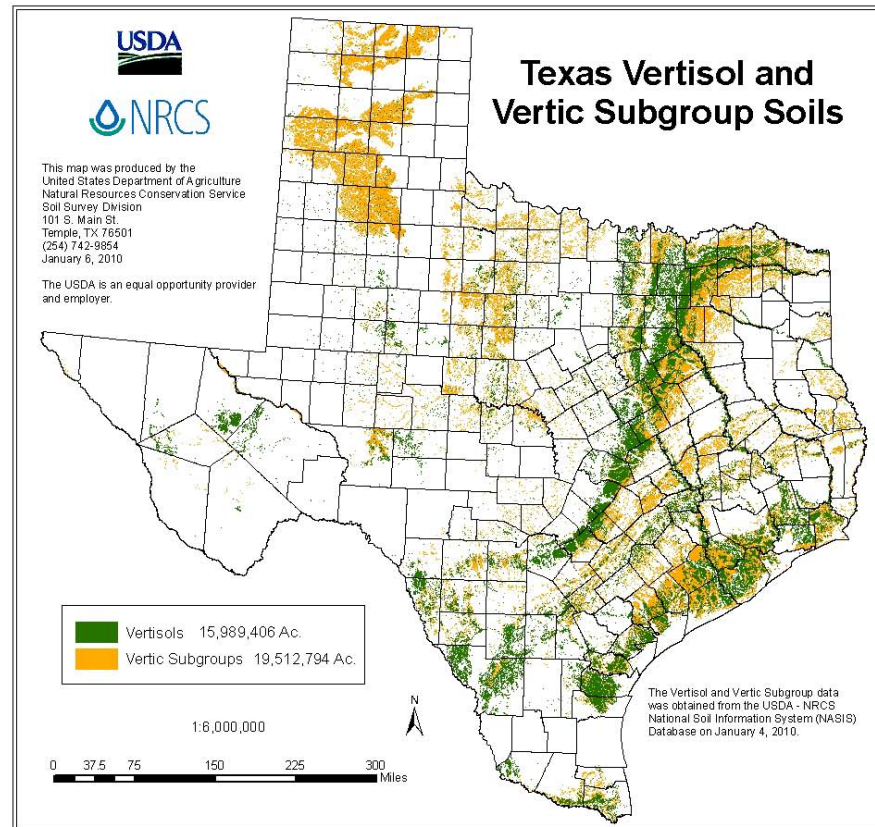


Figure 17: Distribution of soils with high shrink-swell potential in Texas (Vertisols). After USDA.

Shrink-Swell in Soils

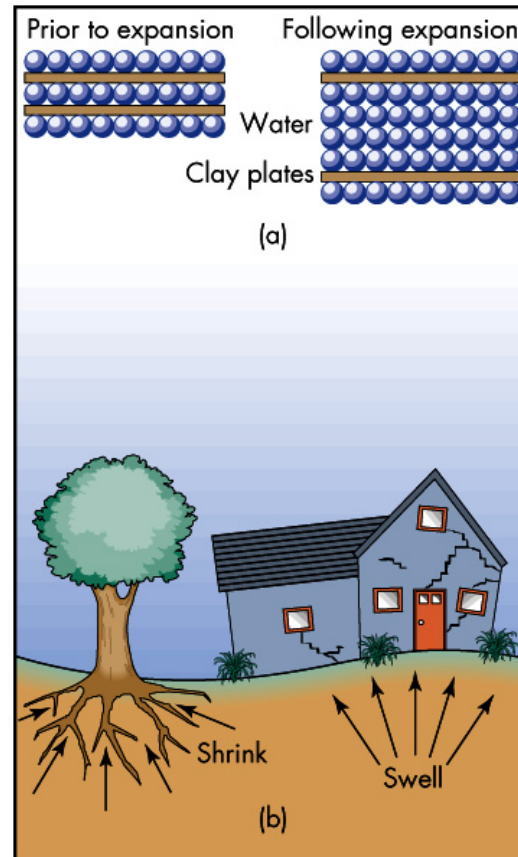


Figure 18: Shrink-swell process in Vertisols, and its consequences [Fig. 17.11a-b, Keller, 2011]

Dallas Sat-Unsat Zone Interaction

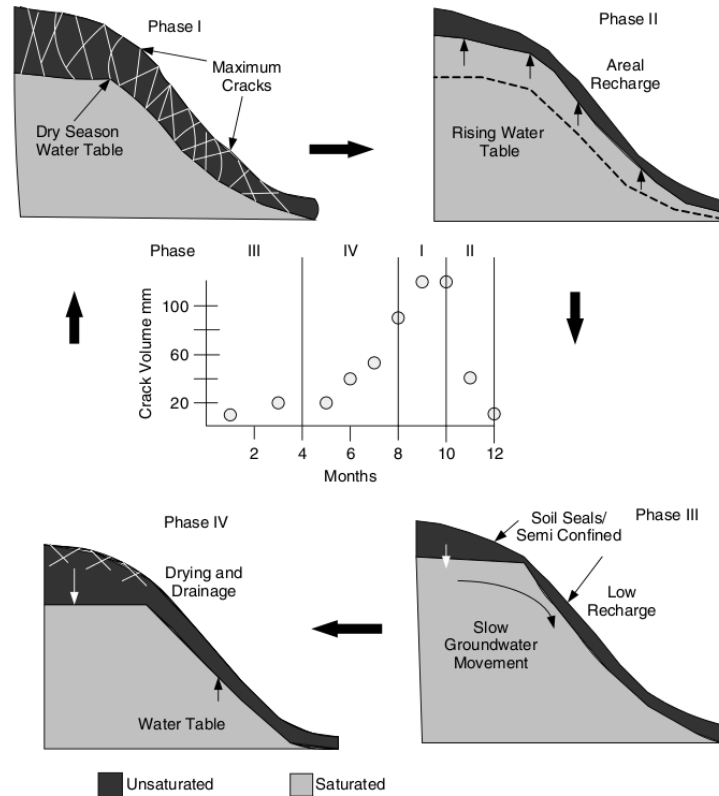


Figure 11. Seasonal phases of soil-aquifer interrelationships for study area

Figure 19: Seasonal changes in aquifer-soil interaction in Blackland Prairie soil [Vertisol, Fig. 11, Allen et al., 2005].

Dallas Sat-Unsat Zone Interaction

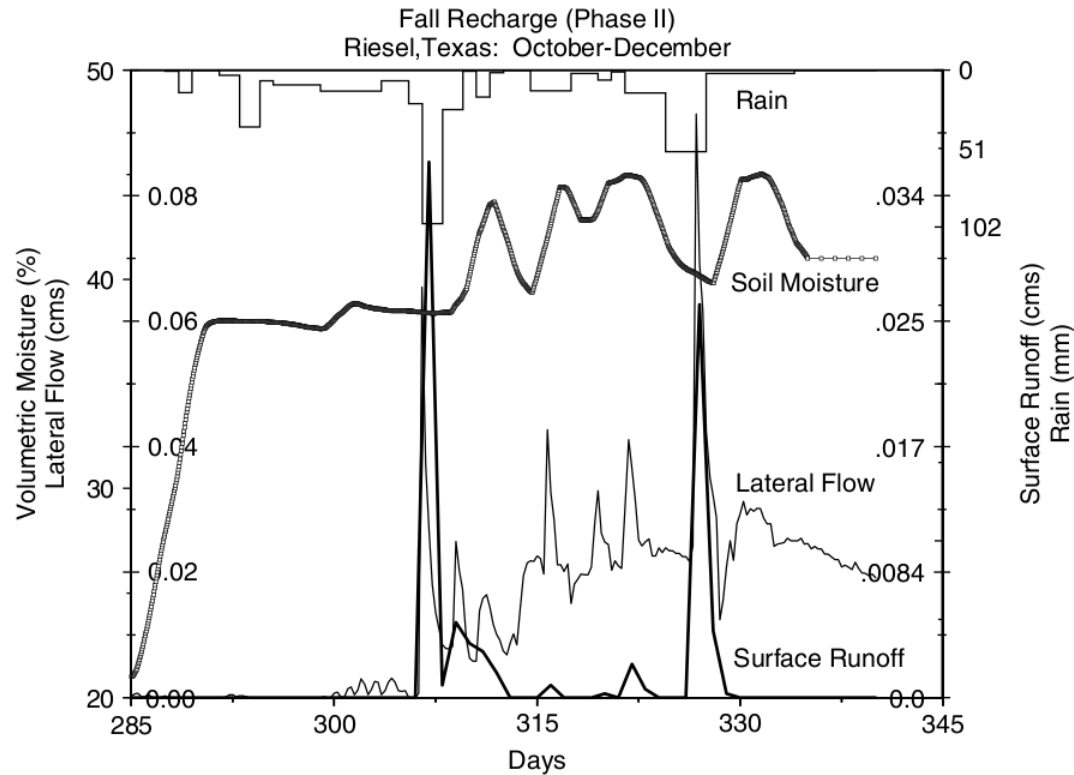


Figure 13. Phase II: fall recharge and rainfall, soil moisture, surface runoff and lateral flow

Figure 20: Seasonal changes in rainfall-runoff in Blackland Prairie soil [Fig. 13, Allen et al., 2005]. This study also found no runoff occurs until 20% of annual rainfall has re-moistened the soil.

Adapting to Climate Change

- As water stress increases, significant changes in agricultural and urban irrigation will be required.
- One method, *surge irrigation* (Fig. 21), enhances crop water efficiency significantly (Fig. 22).
- a casualty of these issues is rice farming in Australia

Surge Irrigation

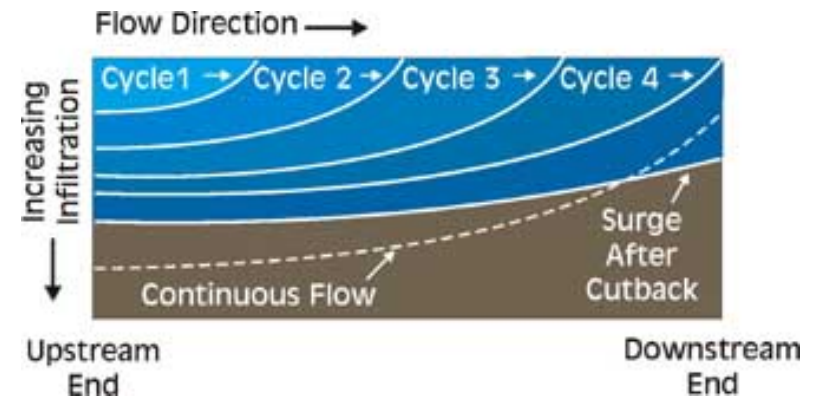
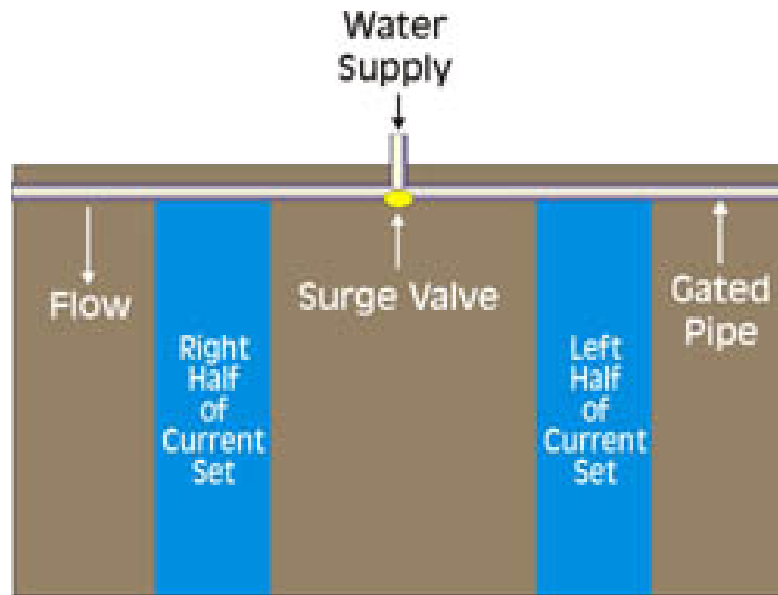


Figure 21: Surge irrigation principles, after U. Neb. Right shows alternating distribution of irrigation surges, left shows resulting soil moisture infiltration.

Surge Efficiency

Table 2. Water productivity (WP) values for the three treatments

Parameters	Treatment ^a					
	Season 1			Season 2		
	I	II	III	I	II	III
Mean yield (t ha ⁻¹)	3.8	7.5	10.1	5.1	8.2	11.0
Water applied per hectare (m ³)	711	5250	6370	7140	5270	6370
Water productivity (kg m ⁻³)	0.53	1.43	1.58	0.71	1.55	1.72

^a Treatment: I, traditional; II, deficit; III surge.

Figure 22: Surge irrigation benefits: increased irrigation efficiency (*water productivity*, or increased crop yield per unit of water). From a study of Vertisol agriculture, Ethiopia [Jiru and Van Ranst, 2010].

Bibliography

PM Allen, RD Harmel, J Arnold, B Plant, J Yelderman, and K King. Field data and flow system response in clay (vertisol) shale terrain, north central Texas, USA. *HYDROLOGICAL PROCESSES*, 19(14):2719–2736, SEP 2005. ISSN 0885-6087. doi: 10.1002/hyp.5782.

C. W. Fetter. *Applied Hydrogeology*. Prentice Hall, Upper Saddle River, NJ, 4th edition, 2001. ISBN 0-13-088239-9.

R. A. Freeze and J. A. Cherry. *Groundwater*. Prentice-Hall, Englewood Cliffs, NJ, 1979.

D. Hillel. *Applications of soil physics*. Academic Press, New York, 1980. ISBN 0-12-348580-0.

Mintesinot Jiru and Eric Van Ranst. Increasing water productivity on Vertisols: implications for environmental sustainability. *JOURNAL OF THE SCIENCE OF FOOD AND AGRICULTURE*, 90(13):2276–2281, OCT 2010. ISSN 0022-5142. doi: 10.1002/jsfa.4082.

W. A. Jury, W. R. Gardner, and W. H. Gardner. *Soil Physics*. John Wiley and Sons, New York, 1991. ISBN 0-471-83108-5.

E. A. Keller. *Environmental Geology*. Prentice Hall, Upper Saddle River, NJ, 8th edition, 2000. ISBN 0-13-022466-9.

E. A. Keller. *Introduction to Environmental Geology*. Prentice Hall, 5th edition, 2011. ISBN 9780321727510. URL <http://www.pearsonhighered.com/educator/product/Introduction-to-Environmental-Geology-5E/9780321727510.page>.

J. Simunek, M. T. van Genuchten, and M. Sejna. Using the hydrus-1d and hydrus-2d codes for estimating unsaturated soil hydraulic and solute transport parameters. In M. T. van Genuchten, F. J. Leij, and L. Wu, editors, *Proceedings of the international workshop on Characterization and measurement of the hydraulic properties of unsaturated porous media*, pages 1733–1738. Dordrecht, CA, 2004. ISBN 1-4020-1888-6.